Iterative Learning Control of Antilock Braking of Electric and Hybrid Vehicles

Chunting Mi, *Senior Member, IEEE*, Hui Lin, and Yi Zhang

***Abstract*—Hybrid electric vehicles (HEVs) use multiple sources of power for propulsion which provides great ease and flexibility to achieve advanced controllability and additional driving performance. In this paper, the electric motor in HEV and electric vehicle (EV) propulsion systems is used to achieve antilock braking performance without a conventional antilock braking system (ABS). The paper illustrates that the antilock braking of HEV can be easily achieved using iterative learning control for various road conditions. A vehicle model, a slip ratio model, and a vehicle speed observer were developed to control the antilock performance of HEV during braking. Through iterative learning process, the motor torque is optimized to keep the tire slip ratio corresponding to the peak traction coefficient during braking. Simulations were performed on a compact size vehicle to validate the proposed control method. The control algorithm proposed in this paper may also be used for the ABS control of conventional vehicles.**

***Index Terms*—Antilock braking system (ABS), electric vehicle, hybrid electric vehicle (HEV), iterative learning control, regenerative braking, road vehicle control, road vehicle electric propulsion, road vehicle electronics, road vehicle power systems, traction control.**

I. Introduction

HYBRID electric vehicles (HEVs) offer remarkable fuel savings and emission reduction. For example, the Toyota Prius HEV offers as high as 60 miles per gallon (mpg) fuel consumption in city driving and 51 mpg in highway driving, while the equivalent model, Corolla, which is driven by an internal combustion engine (ICE) alone, can only achieve 30 mpg in city driving and 38 mpg in highway driving [1]. In recent years, there have been many studies focused on the modeling and control of HEVs [2]–[7].

The use of multiple sources of power in HEVs offers great ease and flexibility to achieve advanced controllability and additional driving performance. One of the advanced features of modern vehicles is the antilock braking system (ABS) and traction control (TC). The purpose of ABS is to optimize the braking effectiveness and maintain vehicle stability, especially in wet or icy road conditions. In conventional vehicles driven by ICE alone, the ABS is achieved through the use of hydraulic systems. The control of ABS is complicated and sometimes may not be effective due to the nonlinear characteristics and unknown environmental parameters. Advanced control algorithms, such as fuzzy logic control [8]–[10], neural network [11], hybrid control [12], adaptive control [13], and other intelligent control [14]–[16] have been developed to achieve antilock braking performance for conventional vehicles.

In the area of HEVs, recent studies have been focused on developing regenerative system models [17], [18], simulation of regenerative braking [19], and motor control [20]. Antilock braking and traction control of pure electric vehicles (EVs) were also investigated [21]–[24].

The use of electric motors in HEV propulsion makes it possible to eliminate the expensive ABS associated with conventional hydraulic brakes. In addition to the primary function of propulsion, the electric motor can also be used effectively as the braking device because of its fast torque response characteristics and capability of regeneration. The fast torque response provides the opportunity to improve the vehicle antilock performance through the control of motor torque, without conventional ABS.

Iterative learning control (ILC) has been proven to be effective for controls related to nonlinear dynamic systems [25]. In this paper, the ILC was proposed to control the antilock braking of EV and HEV, using the electric motor to provide the required braking torque. A vehicle model, a slip ratio model, and a vehicle speed observer were developed and integrated to control the vehicle braking performance under various road conditions, based on ILC theory.

Through the iterative learning process, the control signal, namely, the motor torque, has been optimized so that the tire slip ratio during braking is maintained near the value corresponding to the highest traction force. The proposed approach was applied to a typical compact size vehicle as a case study. Model-based simulation results validated the proposed control method. It is shown that the control algorithm can automatically adjust to various road conditions.

II. Vehicle Model

Fig. 1 shows the one-wheel model of HEV for braking studies, where the wind force, hill climbing force and rolling resistance are neglected. The slip ratio λ is defined as the relative difference between the vehicle speed and the wheel speed

$$\lambda = \frac{V_\omega - V}{V} \tag{1}$$

Manuscript received July 12, 2004; revised October 14, 2004. This work was supported by the Center for Engineering Education and Practice and by the University of Michigan under a Rackham Grant. Review of the paper was coordinated by Dr. M. A. Masrur.

C. Mi is with the Department of Electrical and Computer Engineering, University of Michigan-Dearborn, Dearborn, MI 48128 USA (e-mail: chrismi@umich.edu; mi@ieee.org).

H. Lin is with the Department of Electrical Engineering, Northwestern Polytechnical University, Shaanxi 710072, China (e-mail: linhui@nwpu.edu.cn).

Y. Zhang is with the Department of Mechanical Engineering, University of Michigan-Dearborn, Dearborn, MI 48128 USA (e-mail: anding@umich.edu).

Digital Object Identifier 10.1109/TVT.2004.841552

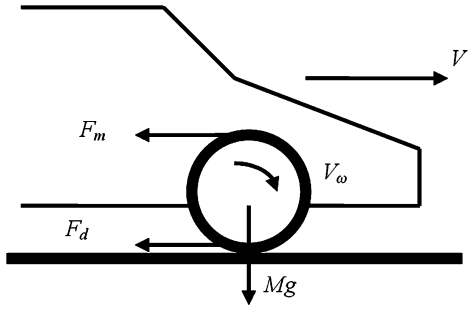

Fig. 1. One-wheel model of vehicles during braking used for ABS study, where $F_{\rm m}$ is the external braking force applied to the wheel by the motor, $F_{\rm d}$ is the braking force caused by tire slip, M is the vehicle mass, and g is the natural acceleration rate.

where V is the vehicle speed and V_ω is the linear speed of the wheel. The wheel speed can be expressed as

$$V_\omega = \omega r \tag{2}$$

where ω is the angular speed of the wheel and r is the radius of the wheel.

During normal driving, $\lambda > 0$, there exists a friction force on the wheel in the direction of the forward motion. This friction force, also known as traction force, is caused by the slip between the road surface and the tire. This force contributes to the forward motion of the vehicle during normal driving. During braking, external forces are applied to the wheel so that the wheel linear speed is less than the vehicle speed, e.g., $\lambda < 0$. Therefore, there exists a friction force opposite to the forward motion.

The traction force or braking force in the case of braking as shown in Fig. 1 can be expressed as

$$F_d(\lambda) = \mu(\lambda) Mg \tag{3}$$

where $\mu(\lambda)$ is the adhesive coefficient between the road surface and the tire and $\mu(\lambda)$ is a function of slip ratio λ.

During braking, the braking force is opposite to the forward motion. When neglecting wind force, rolling resistance, and hill climbing force, the equation of the vehicle motion can be expressed as

$$M\frac{dV}{dt} = -F_d(\lambda). \tag{4}$$

In order to enter braking mode, an external torque must be applied to the wheel to slow down the wheel. In HEV, this torque is the sum of the motor regenerative braking torque and additional braking torque provided by the mechanical braking systems, in case the motor torque is not enough to provide effective braking.

The braking torque applied to the wheel is in the opposite direction of the wheel rotation and slows down the wheel. The traction force, on the other hand, is in the same direction as the wheel rotation and therefore will accelerate the wheel, as shown in Fig. 1. The equation of the wheel motion can be expressed as

$$J_\omega \frac{d\omega}{dt} = -T_m + rF_d(\lambda) \tag{5}$$

where J_ω is the wheel inertia and $T_{\rm m}$ is the total braking torque.

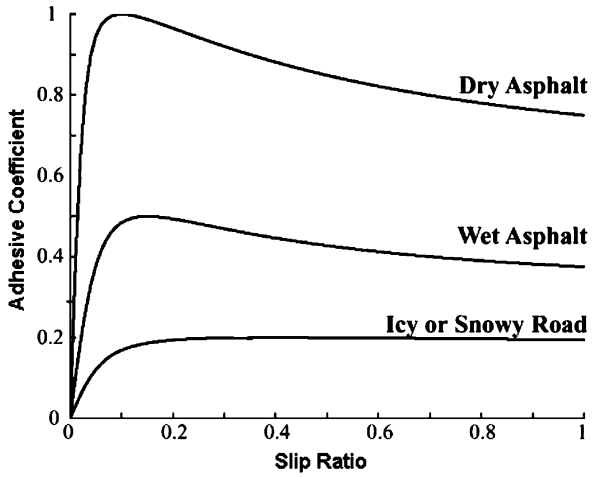

Fig. 2. Typical adhesive coefficient between the road surface and the tires, as a function of slip ratio and road surface conditions.

As stated before, the braking force is a function of the adhesive coefficient between the tire and the pavement. The adhesive coefficient is determined by the road surface, the tire condition, and the slip ratio. Typical road adhesive coefficients are shown in Fig. 2 as a function of road surface and slip ratio [16]. It can be seen from Fig. 2 that the adhesive coefficient reaches maximum value near the slip ratio of $\lambda^* = 0.18$ for most road conditions. When the slip ratio is below λ^*, increasing the slip ratio can increase the traction force. Once the slip ratio exceeds λ^*, the traction force will decrease as a result of the decrease of adhesive coefficient.

III. Slip Ratio Model

Vehicles may brake on any road surface with any tire condition in any environment. The purpose of vehicle antilock braking control is to achieve maximum braking force for all road conditions when a maximum braking effect is demanded by the driver. It can be seen from (4) that, during braking, the vehicle speed is a function of traction force. The traction force itself is a function of slip ratio and the slip ratio is unknown. It can be seen from (5) that the wheel speed can be controlled by properly adjusting the braking torque $T_{\rm m}$.

The wheel slip ratio must be controlled near the optimum value so that maximum traction force can be provided to the wheels during braking while maintaining the stability of the vehicle. In order to control the slip ratio, a slip ratio model needs to be developed.

The slip ratio model can be derived from (1). Taking the derivative of both sides of (1) about vehicle speed V, the following equations can be obtained:

$$\dot{\lambda} = -\frac{1}{V}\dot{V}_\omega + \frac{V_\omega}{V^2}\dot{V} = -(1+\lambda)\frac{\dot{V}}{V} + \frac{1}{V}\dot{V}_\omega \tag{6}$$

where V and λ are functions of time which can be defined as the state space variables

$$\begin{cases} x_1(t) = \lambda \\ x_2(t) = V \end{cases}. \tag{7}$$

From (3) and (4), the derivative of the vehicle speed can be written as

$$\dot{V} = -g\mu(\lambda). \tag{8}$$

Therefore, the following state space functions can be derived using (5)–(8)

$$\begin{cases} \dot{x}_1(t) = (1 + x_1(t)) \frac{g\mu(x_1)}{x_2(t)} + \frac{r^2 M g\mu(x_1)}{x_2(t) J_\omega} - \frac{r}{x_2(t) J_\omega} T_m(t) \\ \dot{x}_2(t) = -g\mu(x_1) \end{cases}. \tag{9}$$

Further, the total braking torque can be controlled proportional to the vehicle speed

$$T_m(t) = x_2(t) u(t) \tag{10}$$

where $u(t)$ is a function to be obtained through ILC.

Substituting (10) to (9), the state space function becomes

$$\begin{cases} \dot{x}_1(t) = (1 + x_1(t)) \frac{g\mu(x_1)}{x_2(t)} + \frac{r^2 M g\mu(x_1)}{x_2(t) J_\omega} - \frac{r}{J_\omega} u(t) \\ \dot{x}_2(t) = -g\mu(x_1) \end{cases}. \tag{11}$$

The slip ratio λ is the output

$$Y(t) = [1, 0] \begin{bmatrix} x_1(t) \\ x_2(t) \end{bmatrix}. \tag{12}$$

The input can also be written as a vector

$$X(t) = [x_1(t), x_2(t)]^T. \tag{13}$$

Then the following state-space functions are obtained

$$\begin{cases} \dot{X}(t) = f(X(t), t) + B(X(t), t) u(t) \\ Y(t) = C(t) X(t) \end{cases} \tag{14}$$

where

$$f(X(t), t) = \left[(1 + x_1(t)) \frac{g\mu(x_1)}{x_2(t)} + \frac{r^2 M g\mu(x_1)}{x_2(t) J_\omega} - g\mu(x_1) \right] \tag{15}$$

$$B(X(t), t) = \left[-\frac{r}{J_\omega}, 0 \right]^T \tag{16}$$

$$C(t) = [1, 0]. \tag{17}$$

The purpose of further study is to find the desired braking torque for any given vehicle speed on any road condition, so that effective braking can be achieved by controlling the slip ratio corresponding to the maximum adhesive coefficient.

IV. Iterative Learning Control

The state space function (14) is a nonlinear differential function. The ILC theory was used to find the optimal braking torque in this paper. The ILC theory states that, for a given system as shown in Fig. 3, there exists an input $u(t)$ such that the output of the process converges to desired output $y_d(t)$; and that $u(t)$ can be obtained through an iterative proportional-integral-derivative (PID) learning algorithm [26]. Based on the ILC theory, (14) converges when a D type or PD type learning algorithms are used [26]. For D algorithm, the $u(t)$ can be written as

$$u_{k+1}(t) = u_k(t) + \Gamma \frac{de_{k+1}(t)}{dt}. \tag{18}$$

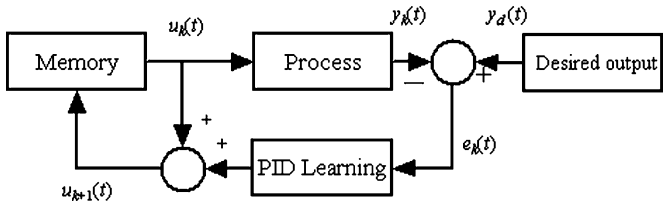

Fig. 3. Iterative learning control.

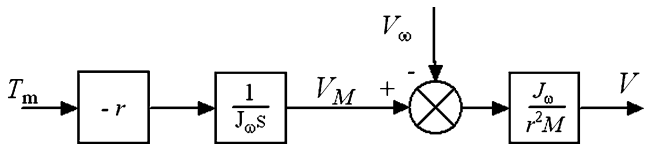

Fig. 4. The vehicle speed observer assuming the wheel speed is measurable.

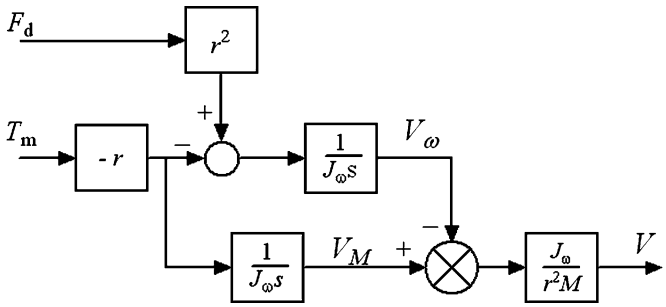

Fig. 5. The actual vehicle speed calculated with a known traction force.

For PD algorithm, $u(t)$ can be written as

$$u_{k+1}(t) = u_k(t) + \Gamma \frac{de_{k+1}(t)}{dt} + \Gamma_p e_{k+1}(t) \tag{19}$$

where

$$e(t) = \lambda_g(t) - \lambda(t) \tag{20}$$

is the error between desired slip ratio and the actual slip ratio; $\lambda_g(t)$ is the desired slip ratio; $\lambda(t)$ is the actual slip ratio; and Γ and Γ_p are learning gain matrixes, respectively. The subscript k denotes the kth step of learning.

From the ILC theory [26], if

$$\rho\left[(1 + \Gamma CB)^{-1}\right] < 1 \tag{21}$$

the learning law expressed by (18) and (19) will converge, where ρ is the spectrum radius and B and C are given in (16) and (17).

V. Vehicle Speed Observer

The wheel speed can be easily detected. The vehicle speed, however, is difficult to directly detect. Therefore, a vehicle speed observer must be established before the learning algorithm can be implemented.

Assuming that the vehicle speed is the same as the wheel speed at the beginning of braking and after braking torque is applied to the wheels, there will be a difference between the wheel

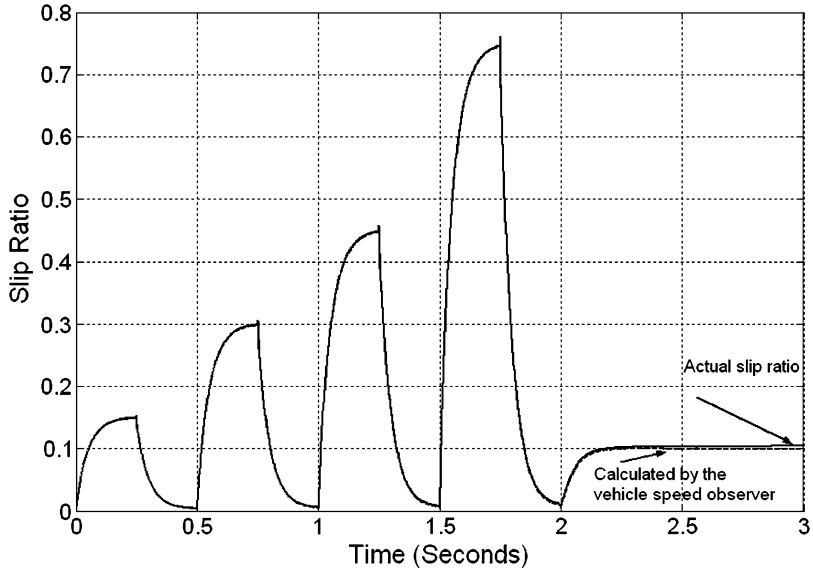

Fig. 6. Comparison of the slip ratio calculated by the proposed vehicle speed observer and calculated using a given traction force.

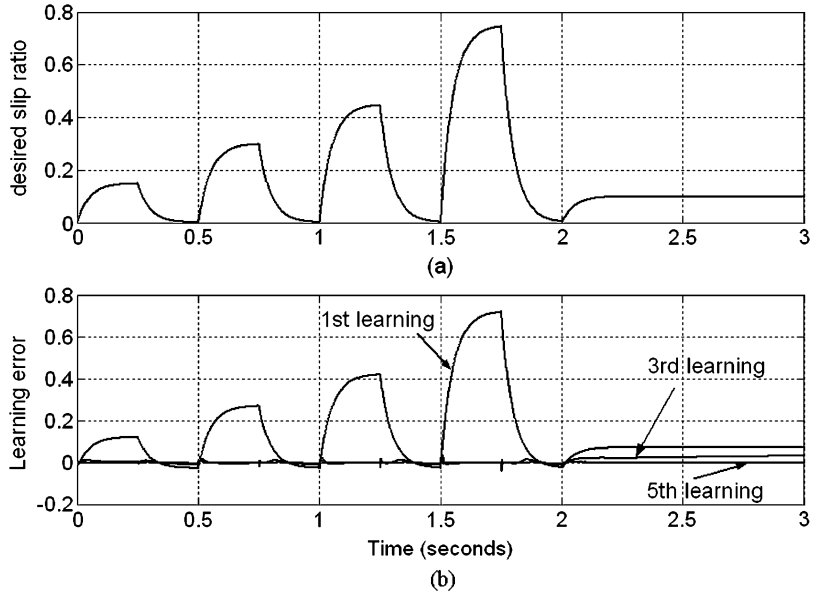

Fig. 7. The learning process. (a) Desired slip ratio and (b) error of each learning step.

speed and the vehicle speed. During braking, when assuming no slip, the wheel kinematic equation can be expressed as

$$\frac{J_\omega}{r}\frac{dV_M}{dt} = -T_m \tag{22}$$

where V_{M} is a model speed when assuming no slip. Integrating (22), this model speed is obtained as

$$V_M(t) = -\int \frac{r}{J_\omega} T_m dt + V_M(0) \tag{23}$$

where $\mathrm{V_M}(t)$ is the model speed at time t and $\mathrm{V_M}(0)$ is the initial model speed at the beginning of braking.

From (2) and (5), the linear speed of the wheel can be derived as

$$V_\omega(t) = \frac{1}{J_\omega}\int (r^2 F_d - rT_m)dt + V_\omega(0) \tag{24}$$

where $\mathrm{V}_\omega(0)$ is the initial wheel speed at the start of braking.

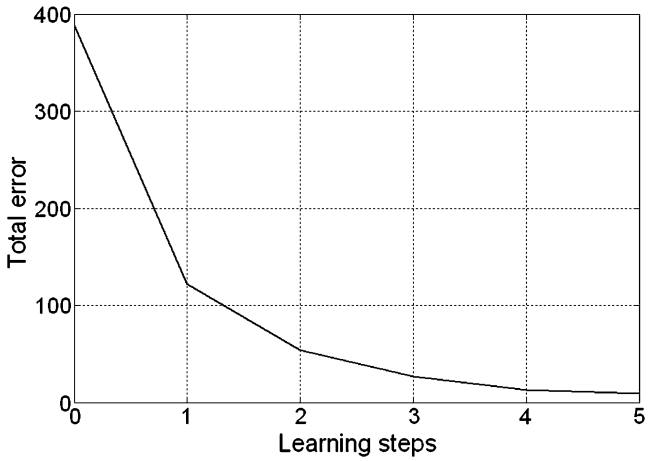

Fig. 8. The total error expressed in $\int |e(t)|dt$.

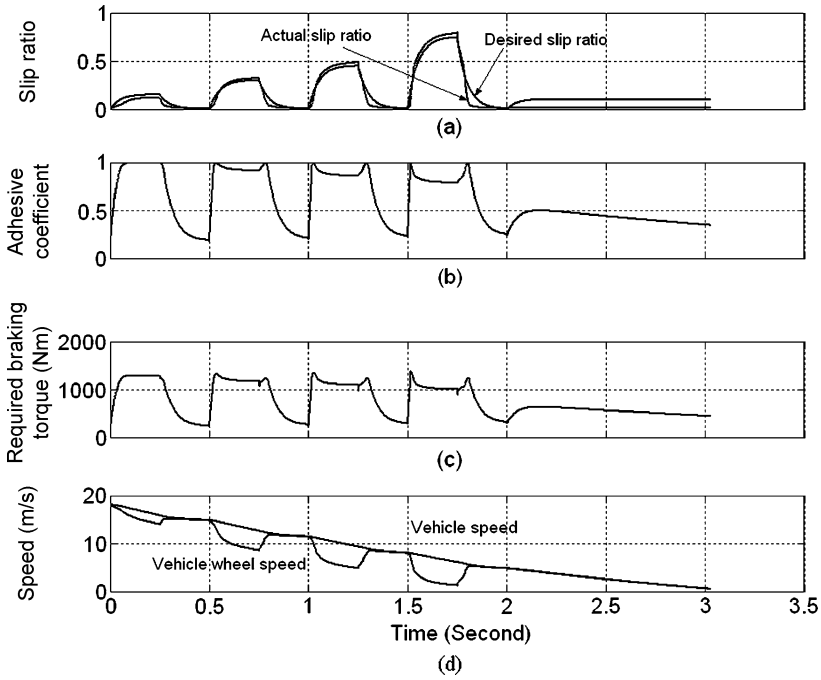

Fig. 9. Braking of the vehicle after the third step of learning. (a) Desired and actual slip ratio, (b) adhesive coefficient, (c) required braking torque, and (d) vehicle speed and wheel speed.

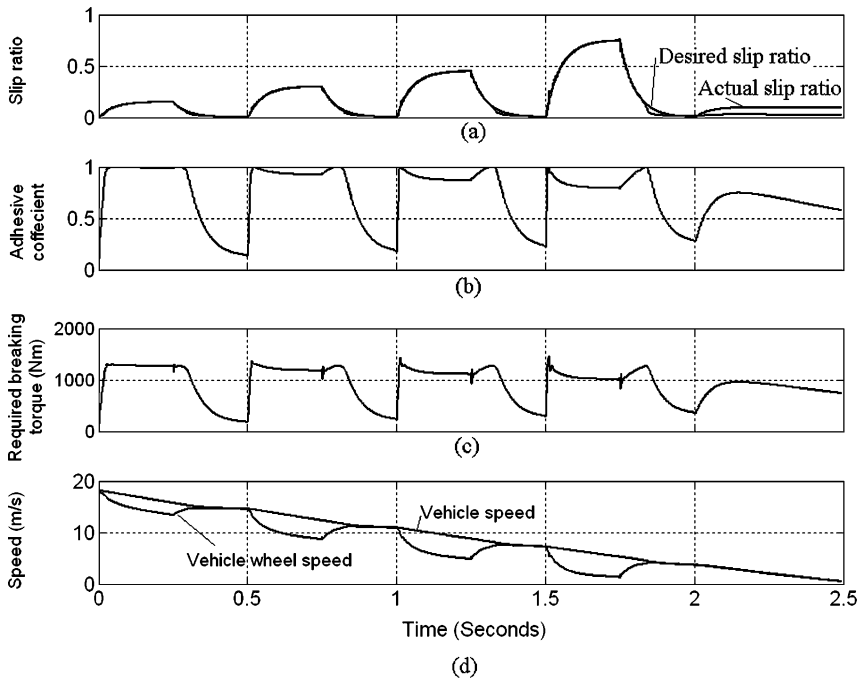

Fig. 10. Braking of the vehicle after the fifth step of learning. (a) Desired and actual slip ratio (overlapped due small error), (b) adhesive coefficient, (c) required braking torque, and (d) vehicle speed and wheel speed.

From (4), the vehicle speed can be obtained by integrating the traction force

$$V(t) = -\frac{1}{M}\int F_d(\lambda)dt + V(0). \tag{25}$$

TABLE I
CONSTANTS FOR THE CONTROLLER INPUT FUNCTION

CONSTANTS	b_1	b_2	b_3	b_4
Value	-130.99	0.54471	115.14	0.29713

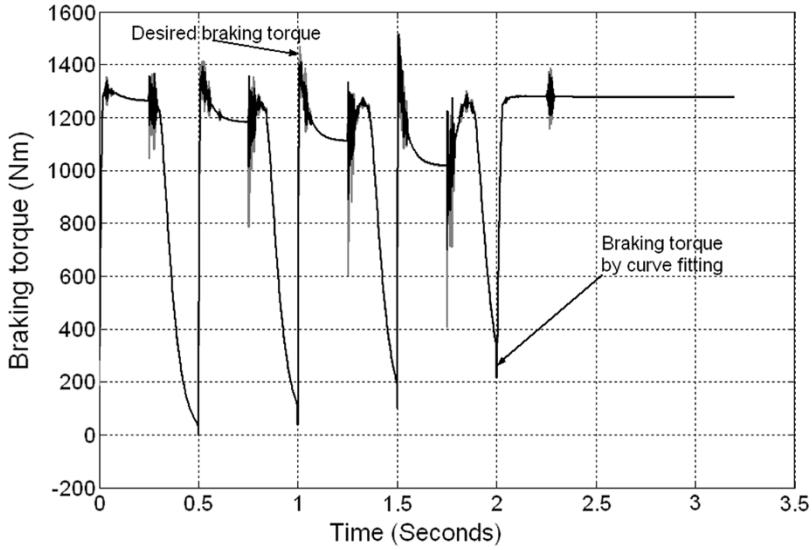

Fig. 11. Comparison of the curve fitting results with the desired motor torque.

However, the traction force is a function of slip ratio and is unknown. Therefore, the vehicle speed can only be observed by eliminating the traction force. Substituting (23) and (24) into (25), the vehicle speed can be derived

$$V(t)=\frac{J_\omega}{r^2M}[V_M(t)-V_\omega(t)]-\frac{J_\omega}{r^2M}[V_M(0)-V_\omega(0)]+V(0). \tag{26}$$

At the beginning of braking, $t=0$. By substituting $t=0$ to (26), the initial vehicle speed can be derived

$$V(0)=\frac{J_\omega}{r^2M}[V_M(0)-V_\omega(0)]. \tag{27}$$

Substituting (27) to (26), the vehicle speed can be obtained

$$V(t)=\frac{J_\omega}{r^2M}[V_M(t)-V_\omega(t)]. \tag{28}$$

Since the wheel speed can be easily measured, the vehicle speed observer can be constructed from (23) and (28) as shown in Fig. 4. The accuracy of the proposed vehicle speed observer can be validated if the traction force is known. Fig. 5 shows the vehicle speed calculated with a known traction force. Fig. 6 compares the slip ratio calculated by the vehicle speed observer and the actual vehicle speed obtained from Fig. 5. It can be seen that the error is negligible.

VI. The Iterative Learning Process

In order to obtain the required braking torque for desired braking performance, a desired slip ratio, as shown in Fig. 7(a), was constructed for the learning process. Various road conditions and vehicle speeds were studied.

The ILC algorithm was implemented using Matlab. The error between the desired slip ratio and the actual slip ratio for different learning steps is shown in Fig. 7(b) for a dry road surface, with initial vehicle speed of 65 km/h. It can be seen from Fig. 7 that after the first step of learning, the error is very big because the actual slip ratio is almost zero. After the fifth step of learning, the error approaches zero as the actual slip ratio approaches the desired slip ratio. The total error was calculated using $\int |e(t)|dt$ and shown in Fig. 8. After the fifth step of learning, the actual slip ratio well follows the desired slip ratio. The vehicle performance after the third and the fifth learning steps is shown in the Figs. 9 and 10, respectively.

TABLE II
Vehicle Parameters

Parameters	Symbol	Value
Vehicle Mass (kg)	M	1300
Wheel Radius (m)	r	0.3
Rotating Inertia (kg.m^2)	J	0.55
Shaft Gearing ratio	a	3
Maximum Motor torque (Nm)	$T_{\rm m}$	300

VII. Construction of Required Braking Torque

The optimal control was obtained based on the iterative learning law (18) or (19). It can be seen from Fig. 10 that the required braking torque $T_m(t)$ is a function of slip ratio and vehicle speed. When the desired slip ratio $\lambda_g(t)$ or the vehicle speed change, the system has to repeat the learning process.

Therefore, it is necessary to construct an appropriate control law so that it can satisfy various operation conditions. In this paper, the braking torque was constructed as the following:

$$T_m(t)=b_1\dot{V}(t)+\left[b_2\dot{\lambda}_g(t)+b_3e(t)+b_4\dot{e}(t)\right]V(t) \tag{29}$$

where $e(t)$ is the difference between the desired slip ratio and the actual slip ratio defined in (20); b_1, b_2, b_3, and b_4 are constants determined by curve fitting based on optimal braking torque $T_m(t)$ of the fifth learning step.

By using the required braking torque obtained in Fig. 10, and through curve fitting using (29), the constants in (29) can be obtained as shown in Table I. Fig. 11 shows a comparison between the required braking torque and the constructed braking torque. It can be seen that the discrepancy is negligible.

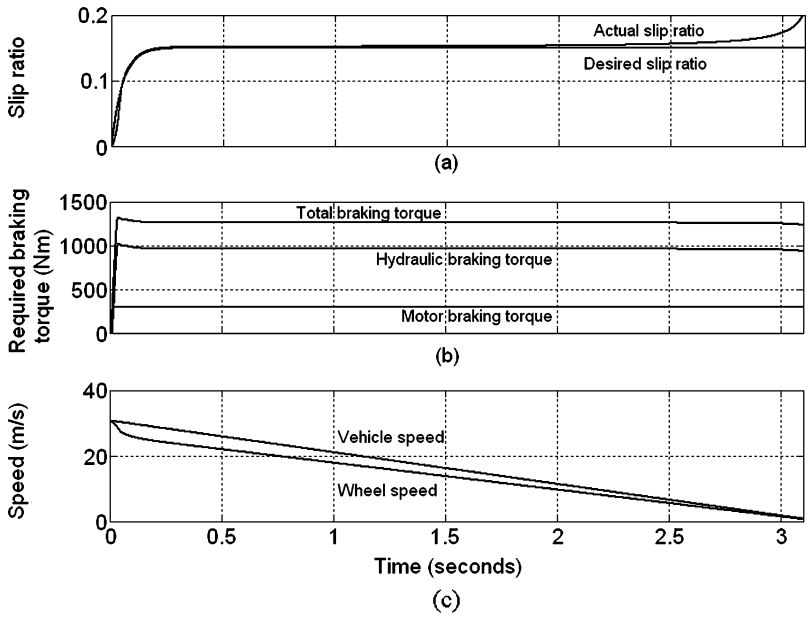

Fig. 12. Vehicle speed during braking for given driving cycle: initial speed 110 km/h, dry asphalt surface. Total braking time is 3 s. (a) Desired slip ratio and actual slip ratio, (b) required braking torque, and (c) vehicle speed and wheel speed.

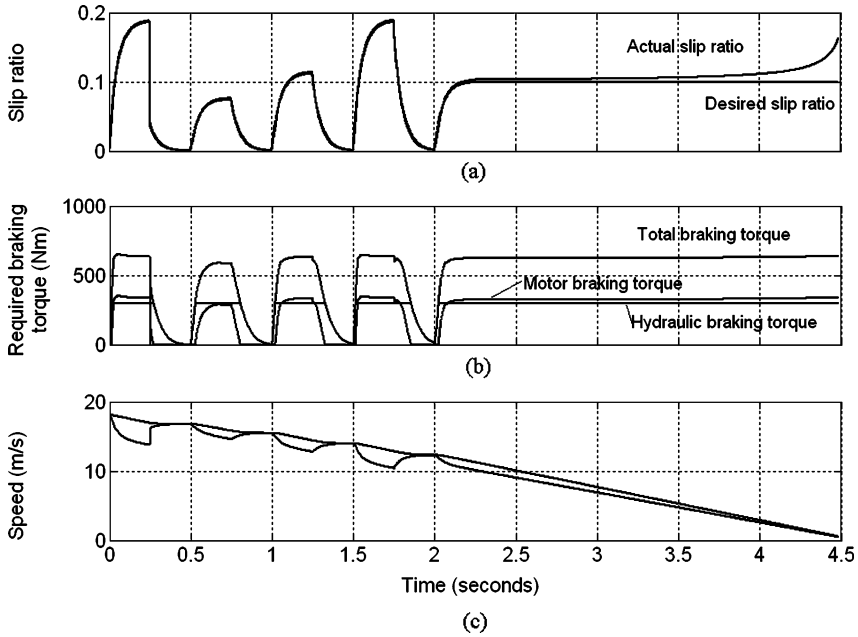

Fig. 13. Vehicle speed during braking for given driving cycle: initial speed is 65 km/h, wet asphalt surface. Total braking time is 4 s. (a) Desired slip ratio and actual slip ratio, (b) required braking torque, and (c) vehicle speed and wheel speed.

VIII. Case Studies

The proposed method was used to simulate the braking of a compact size vehicle for different driving cycles and road conditions. Table II shows the vehicle parameters used in these case studies.

For a dry road surface and an initial vehicle speed of 110 km/h, if maximum braking effect is demanded by the driver, the desired slip ratio should be set to 0.18. The simulation showed that the braking time is within 3 s as shown in Fig. 12. It can be seen from Fig. 12 that in order to achieve this kind of fast braking, approximately 1000 Nm of braking torque is needed. The motor along can only supply 300 Nm of torque. The rest must be provided by the hydraulic braking system.

For a wet road surface, given initial vehicle speed of 65 km/h, the desired slip ratio was set to vary as shown in Fig. 13, to simulate a driver's demand for braking. The braking time is 4.5 s.

For an icy road surface, given initial vehicle speed of 110 km/h, the desired slip ratio was set to 0.16. Due to the low adhesive force provided by the icy road surface, the motor is able to provide the required braking torque. However, the braking time increases to 16 s, as shown in Fig. 14.

It can be seen from Figs. 12–14 that for all road conditions and initial vehicle speeds, the actual slip ratio well follows the

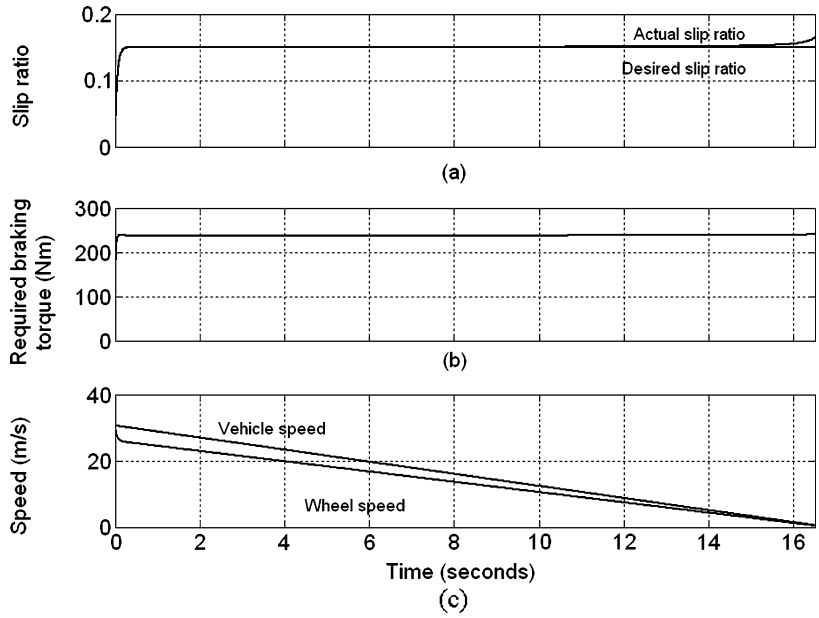

Fig. 14. Vehicle speed during braking for given driving cycle: initial speed 110 km/h, icy asphalt surface. Total braking time is 16 s. (a) Desired slip ratio, actual slip ratio and adhesive coefficient, (b) required braking torque, and (c) vehicle speed and wheel speed.

desired slip ratio. Therefore, effect antilock braking performance of HEV can be achieved using (29) for various road conditions and vehicle speeds.

IX. Conclusion

This paper presented an ILC-based approach for the robust antilock braking control of EV and HEV using the electric motor as a braking device. A vehicle model, a slip ratio model, and a vehicle speed observer were developed. The required braking torque of an EV or HEV can be constructed as a function of the vehicle speed, the desired slip ratio, and the actual slip ratio. The key advantage is that, once learned, the controller has the ability to automatically adjust to various road conditions, particularly in wet and icy road conditions. With some modifications, the proposed control algorithm can also be applied to the ABS control of conventional vehicles.

References

[1] "Toyota vehicle specifications,", http://www.toyota.com/vehicles/2005/prius/specs.html; http://www.toyota.com/vehicles/2005/corolla/specs.html, Oct. 18, 2004.

[2] T. W. Tsai, G. Shultz, and N. Higuchi, "A novel parallel hybrid transmission," *J. Mech. Design Trans. ASME*, vol. 123, no. 2, pp. 161–168.

[3] B. K. Powell, K. E. Bailey, and S. R. Cikanek, "Dynamic modeling and control of hybrid electric vehicle powertrain systems," *IEEE Contr. Syst. Mag.*, vol. 18, no. 5, pp. 17–33.

[4] K. L. Butler, M. Ehsani, and P. Kamath, "A Matlab-based modeling and simulation package for electric and hybrid electric vehicle design," *IEEE Trans. Veh. Technol.*, vol. 48, no. 6, pp. 1770-–1118, 1999.

[5] G. Rizzoni, L. Guzzella, and B. M. Baumann, "United modeling of hybrid electric vehicle drivetrains," *IEEE/ASME Trans. Mechatronics*, vol. 4, no. 3, pp. 246–257, Sep. 1999.

[6] X. He and J. W. Hodgeson, "Modeling and simulation for hybrid electric vehicles, I. Modeling," *IEEE Trans. Intell. Transp. Syst.*, vol. 3, no. 4, pp. 235–243, Dec. 2002.

[7] N. J. Schouten, M. A. Salman, and N. A. Kheir, "Fuzzy logic control for parallel hybrid vehicles," *IEEE Trans. Contr. Syst. Technol.*, vol. 10, no. 3, pp. 625–632, 2002.

[8] C. M. Lin and C. F. Hsu, "Self learning fuzzy sliding mode control for antilock braking systems," *IEEE Trans. Contr. Syst. Technol.*, vol. 11, pp. 273–278, Mar. 2003.

[9] D. E. Nelson, R. Challoo, R. A. McLauchlan, and S. I. Omar, "Implementation of fuzzy logic for an antilock braking system," in *1997 IEEE Int. Conf. Systems, Man, and Cybernetics "Computational Cybernetics and Simulation"*, vol. 4, Oct. 1997, pp. 3680–3685.

[10] W. Y. Wang, K. C. Hsu, T. T. Lee, and G. M. Chen, "Robust sliding mode-like fuzzy logic control for anti-lock braking systems with uncertainties and disturbances," in *Int. Conf. Machine Learning Cybernetics*, vol. 1, Nov. 2003, pp. 633–638.

[11] C. M. Lin and C. F. Hsu, "Neural-network hybrid control for antilock braking systems," *IEEE Trans. Neural Netw.*, vol. 14, pp. 351–359, Mar. 2003.

[12] T. A. Johansen, J. Kalkkuhl, J. Ludemann, and I. Petersen, "Hybrid control strategies in ABS," in *Proc. 2001 Amer. Control Conf.*, vol. 2, Jun. 2001, pp. 1704–1705.

[13] J. S. Yu, "A robust adaptive wheel-slip controller for antilock brake system," in *Proc. 36th IEEE Conf. Decision Control*, vol. 3, Dec. 1997, pp. 2545–2546.

[14] S. Drakunov, U. Ozguner, P. Dix, and B. Ashrafi, "ABS control using optimum search via sliding modes," *IEEE Trans. Contr. Syst. Technol.*, vol. 3, pp. 79–85, Mar. 1995.

[15] W. K. Lennon and K. M. Passino, "Intelligent control for brake systems," *IEEE Trans. Contr. Syst. Technol.*, vol. 7, pp. 188–202, Mar. 1999.

[16] P. E. Wellstead and B. B. O. L. Pettit, "Analysis and redesign of an antilock brake system controller," *Proc. Inst. Elect. Eng. Control Theory Applicat.*, vol. 144, no. 5, pp. 413–426, Sept. 1997.

[17] M. Panagiotidis, G. Delagrammatikas, and D. Assanis, "Development and use of a regenerative braking model for a parallel hybrid electric vehicle," in *SAE 2000 World Congr.*, Detroit, MI, 2000, SAE paper 2000-01-0995.

[18] S. R. Cikanek and K. E. Bailey, "Regenerative braking system for a hybrid electric vehicle," in *Proc. Amer. Control Conf.*, Anchorage, AK, May 2002, pp. 3129–3134.

[19] H. Yeo and H. Kim, "Hardware in the loop simulation of regenerative braking for a hybrid electric vehicle," in *Proc. Inst. Mech. Eng.*, vol. 216, 2002, pp. 855–864.

[20] H. Gao, Y. Gao, and M. Ehsani, "A neural network based SRM drive control strategy for regenerative braking in EV and HEV," in *IEEE Int. Conf. Electric Machines Drives (IEMDC 2001)*, 2001, pp. 571–575.

[21] P. Khatun, C. M. Bingham, N. Schofield, and P. H. Mellor, "Application of fuzzy control algorithm for electric vehicle antilock braking/traction control systems," *IEEE Trans. Veh. Technol.*, vol. 52, pp. 1356–1364, Sep. 2003.

[22] ——, "An experimental laboratory bench setup to study electric vehicle antilock braking/ traction systems and their control," in *Proc. IEEE 56th Vehicular Technology Conf.*, vol. 3, Sep. 2002, pp. 1490–1494.
[23] Y. Hori, Y. Toyoda, and Y. Tsuruoka, "Traction control of electric vehicle: basic experimental results using the test EV 'UOT Electric March'," *IEEE Trans. Ind. Appl.*, vol. 34, pp. 1131–1138, Sep. 1998.
[24] S. Sakai, H. Sado, and Y. Hori, "Anti-skid control with motor in electric vehicle," in *Proc. 6th Int. Workshop Advanced Motion Control*, Apr. 2000, pp. 317–322.
[25] Y. C. Wang, C. J. Chien, and C. C. Teng, "Direct adaptive iterative learning control of nonlinear systems using an output-recurrent fuzzy neural network," *IEEE Trans. Syst., Man, Cybern. B, Cybern.*, vol. 34, pp. 1348–1359, Jun. 2004.
[26] H. Lin and L. Wang, *Iterative Learning Control Theory* (in Chinese) Xi'an, Shaanxi, China, 1998, .

Chunting Mi (S'00–A'01–M'01–SM'03) received the B.S.E.E. and M.S.E.E. degrees from Northwestern Polytechnical University, Xi'an, China, and the Ph.D degree from the University of Toronto, Toronto, ON, Canada, all in electrical engineering.

He is an Assistant Professor at the University of Michigan, Dearborn, with teaching responsibilities in the area of power electronics, electric vehicles, electric machines, and electric drives. He joined General Electric Canada Inc. as an electrical engineer in 2000, responsible for designing and developing large electric motors and generators. He started his career in 1988 at the Rare-Earth Permanent Magnet Machine Institute of Northwestern Polytechnical University. He joined Xi'an Petroleum Institute as an Associate Professor and Associate Chair of the Department of Automation in 1994. He was a Visiting Scientist at the University of Toronto from 1996 to 1997. He has recently developed a Power Electronics and Electrical Drives Laboratory at the University of Michigan-Dearborn. His research interests are electric drives, power electronics, induction motors, brushless motors, and PM synchronous machines; renewable energy systems; and electrical and hybrid vehicle powertrain design and modeling.

Dr. Mi is Chair of the Power Electronics and Industrial Electronics Chapter of the IEEE Southeast Michigan Section.

Hui Lin received the B.S.E.E. and M.S.E.E. degrees in electrical engineering and the Ph.D. degree in control science engineering from Northwestern Polytechnical University, Xi'an, China, in 1982, 1985, and 1993, respectively.

He is a now Professor at the Department of Electrical Engineering, Northwestern Polytechnical University. His teaching responsibilities and research interests are in the areas of power electronics, electric vehicles, motion control, and control theory. He was an Associate Chair of the Department of Automation from 1994 to 2001. He was a Visiting Scientist at the Technical University of Braunschweig, Germany, from 1989 to 1990, and at the University of Michigan-Dearborn from 2003 to 2004.

Yi Zhang received the B.S. degree from Central South University, China, in 1982 and the M.S. and Ph.D. degrees from the University of Illinois at Chicago in 1986 and 1989, respectively, all in mechanical engineering.

He joined the University of Michigan-Dearborn in 1992 and is currently an Associate Professor of mechanical engineering. His teaching and research interests are in the areas of gear design and manufacturing, theory of gearing, mechanical design, and vehicle powertrains. His research interests in recent years have been focused on the design, modeling, and control of various types of vehicle transmissions. He has published more than 40 technical papers in gear design and power transmission areas.

Dr. Zhang is a member of ASME.